# Color-Base Damage Feature Enhanced Support Vector Classifier for Monitoring Quake Image

Takato Yasuno(✉), Masazumi Amakata, Junichiro Fujii, and Yuri Shimamoto

Research Institute for Infrastructure Paradigm Shift, Yachiyo Engineering Co., Ltd., CS-Tower, 5-20-8 Asakusabashi, Taito-ku, Tokyo 111-8648, Japan
{tk-yasuno, amakata, jn-fujii, yr-shimamoto}@yachiyo-eng.co.jp

**Abstract.** In recent times, significant natural disasters have affected our city lives. This includes the occurrence of large earthquakes that have devastated the city's infrastructure. During such times of crisis, it is important that emergency response times be as quick as possible to mitigate harm and loss. To achieve this, priority must be given to the various types of initial emergency response. Color image monitoring has the potential to prioritize responses. It uses multi-mode data resources such as openly sourced photos on social media, smartphone cameras, CCTV, and so forth. This paper presents a method to enhance the damaged color features extracted based on a pre-trained deep architecture DenseNet-201 in order to classify damage caused by several earthquakes, whose classifiers are Bayesian optimized to minimize the loss function with cross-validation. This method is applied to a case study of an earthquake image dataset. The study incorporates five target categories, namely bridge collapse, initial smoke and fire, road damage with accident risk to expand secondary loss for relevant users, tsunami damage, and non-disaster. Some advantages have been found when using color feature extraction for monitoring quake damage and further opportunities are remarked (189 words).

**Keywords:** Quake image monitoring · Color-base augmentation · DenseNet-201 · Damage feature enhancement · Support vector classifier

## 1 Introduction

### 1.1 Related Papers and Damage Color Imaging

**Disaster Damage Monitoring and Color Image Sources**

Manzhu et al. [1] reviewed the major sources of big data, the associated achievements in disaster management phases to monitor and detect natural hazards, methods to mitigate against disaster-related damage, and the recovery and reconstruction processes. This study focuses on the urgent response phase after an earthquake, which monitors and detects damage and allows for make decisions in order to address initial


S. Tominaga et al. (Eds.): CCIW 2019, LNCS 11418, pp. 260–275, 2019.
https://doi.org/10.1007/978-3-030-13940-7_20

rapid actions regarding high-priority infrastructures such as roads, intersections, bridges, river gates, and public facilities. Between 2014 and 2016, several data sources were observed in articles, during a time when big data was a popular topic in disaster management. These data sources included satellite, social media, crowd-base data source, sensor web and IoT, mobile GPS, simulation, unmanned aerial vehicles (UAVs), light detection and ranging (LiDAR). Among these digital data sources, satellite imagery [2, 3] and social media [4, 5] data serve as the most popular type of data for disaster management.

However, satellites used for remote sensing travel at slow speeds and contain an interval gap in the data spanning from the previous flyover to the subsequent flyover. These photographs are not sequential causing delay when trying to recognize features of an earthquake disaster. Through the use of social media, spatial temporal sentiment analysis is possible. However, this is prone to inaccuracies because users of social media do not always monitor the disaster damage consistently. Witnesses to a natural disaster will prioritize their well-being and seek safety and shelter after an earthquake resulting in inconsistent data. Messaging is found to occasionally lack essential signals owing to noise, resulting in misinformation. This study focuses on the damaged color image source for monitoring the disaster damage of critical infrastructures to efficiently decide which high-priority responses to undertake them.

**Color-Base Segmentation and Color Feature Augmentation**

Regarding color-based image segmentation using K-means clustering, many proposals and experimental results have been reported. Chitade [6] presented an image segmentation for satellite imagery based on color features in two stages where enhancement of color separation used decorrelation stretching and then grouped the regions into five classes using the K-means clustering algorithm to convert image from RGB to L*a*b* color space. The source claimed that it is possible to reduce the computational cost avoiding feature calculation for every pixel in the image. However, the source focused only on the satellite imagery for mapping the changes of color-base land cover to classify land use pattern. Shmmala [7] compared three versions of K-means clustering algorithms for biological images and ordinary full-colored images under RGB and L*a*b* spaces. Hassan et al. [8] attempted to find the optimal parameter K automatically, and therefore created segmentation without any human supervision to the algorithm. Then, they applied the algorithm to several types of images including flowers, birds, fruits, and games having funs. They presented the combined segmentation of RGB and HSV color spaces, which yielded more accurate results compared to that of a single color space. This combined case had the disadvantage of requiring twice the calculation costs; further, both color spaces are device-dependent.

However, there is currently no approach that is focused on using images of disasters for monitoring damage, and a method of damage color segmentation has not yet been reported to be used as an input for the enhancement of damage feature extraction. Adding the original images with such damage feature extraction using color-based segmentation could enhance the damage features, thereby improving the accuracy of classifier incorporating with color-base saliency enhancement more than that of classifier using the original images. This paper presents a method to enhance the damaged color-base feature extracted based on a pre-trained deep architecture in order to classify

several types of damage after a disaster event, whose classifiers are Bayesian optimized to minimize the loss function with cross-validation. This method is applied to a case study of an earthquake image dataset. Five target classes, namely bridge collapse, initial smoke and fire, road damage with accident risk to expand secondary loss for relevant users, tsunami damage, and non-disaster are incorporated.

## 2 Damage Color Imaging Application

### 2.1 Earthquake Damage Image Dataset

With regard to disaster image datasets, the NOAA [9] provides a natural hazard image database with 1,163 photo images of 67 events of earthquakes that have occurred in the past 100 years from 1915 to 2015. It provides a gallery view of images of each earthquake event. The database includes earthquake disaster images from the USA, Mexico, Guatemala, Colombia, Nicaragua, Peru, Chile, Haiti, Ecuador, Russia, Iran, Turkey, Pakistan, Algeria, Romania, Italy, Papua New Guinea, Australia, New Zealand, Samoa, China, Indonesia, Taiwan, and Japan. However, the quality of the image differs for instances where low-resolution satellite images are used, airplane flight downward view is used, the angle of some photos is on the outdoor and indoor and front of the crushed house. Their region of interests and angles are different and the almost private historical photo collected wisdom without any unified rule. Each earthquake event has limited images; these ones consist of only few disaster images at each earthquake events on that database. Almost all these images are recorded after the earthquakes have occurred, when it has taken more than one week for an international academic survey to obtain relevant lesson historically. We attempted to collect openly source web pages from where the earthquake damage images could be downloaded.

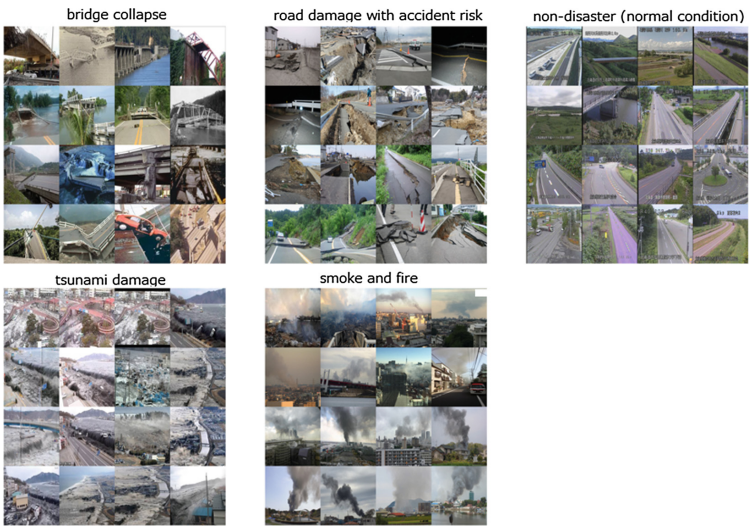


**Fig. 1.** Thumbnail of disaster color image: QuakeV dataset with 16 chosen examples.

This paper highlights the five features of earthquake disasters, namely tsunami damage, bridge collapse, road damage with accident risk, initial smoke and fire, and non-disaster. The authors collected a total number of 1,117 earthquake disaster feature images featured in the datasets. Herein, we focus on earthquake damage features among the color images, and we propose a dataset called QuakeV. Figure 1 shows the thumbnail of the earthquake damage image dataset with validation data that comprised 16 chosen images of each class: tsunami damage, bridge collapse, road damage with accident risk, initial smoke and fire, and non-damage.

## 2.2 Damage Color Feature Extraction

**L*a*b* Color Space Transformation from RGB**

Several color spaces exist for color image representations; some spaces are device-dependent and the other spaces are device-independent. The former includes the RGB, NTSC, YCbCr, HSV, CMY, CMYK, and HSI spaces; these spaces represent color information in ways that are more intuitive or suitable for a particular application. For example, the appearance of RGB colors varies with display and scanner characteristics, and CMYK colors vary with printer, ink, and paper characteristics [10]. These device-dependent color spaces are not the preferred choice for disaster monitoring. This is because the color imaging system does not achieve a sufficient consistency in pre-trained detectors or classifiers required to predict target images. In contrast, one of the

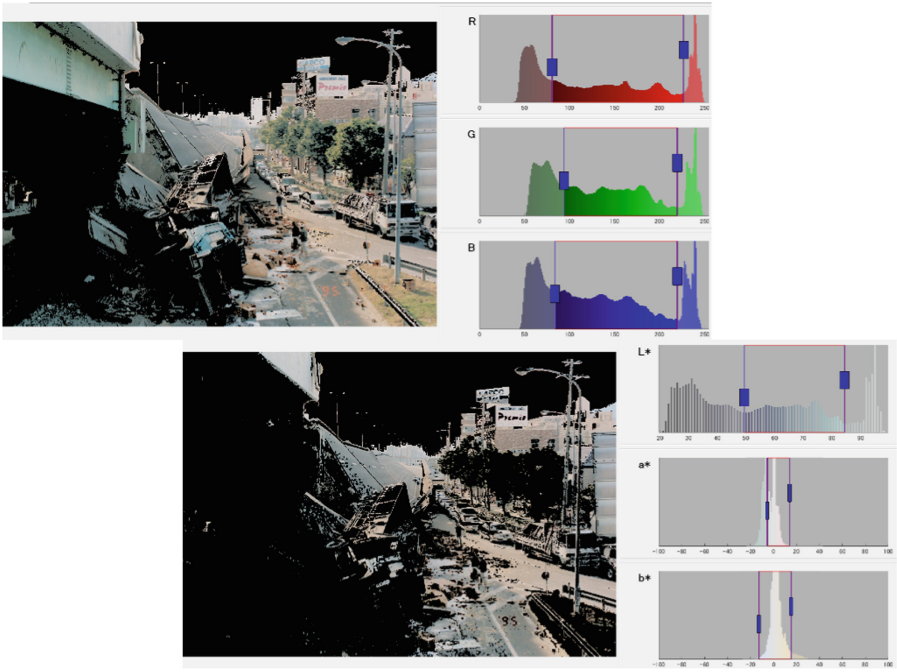


**Fig. 2.** Thresholding three components to mask the background based on RGB (top) and L*a*b* (bottom), photo of the Great Hanshin Awaji Earthquake using the Kobe open data.

most widely used device-independent color spaces is the 1931 CIE XYZ color space developed by Commission Internationale de l'Eclairage (CIE). The CIE has developed additional color space specifications that are better suited to some purposes than XYZ. For example, these include the xyY, uvL, L*a*b*, and L*ch, and sRGB spaces. These device-independent color spaces are supported by the Image Processing Toolbox [11]. The L*a*b* color space was introduced in 1976, and is widely used in color science as well as the design of color devices such as printers, cameras, and scanners. The L*a*b color space provides two key advantages over XYZ as a working space. First, L*a*b* more clearly separates gray-scale information represented as L* values from color information represented using a* and b* values. Second, the L*a*b* was designed so the Euclidean distance in this space corresponds reasonably well with perceived differences between colors. Because of this property, the L*a*b* color space is perceptually uniform. As a corollary, L* values relate linearly to human perception of brightness [11].

The device-independent color space is suited to disaster monitoring. This study uses the L*a*b* color space to take advantage of this trait. Figure 2 shows the thresholding three components on two color spaces such as RGB (top) and L*a*b* (bottom), photo of the Great Hanshin Awaji Earthquake [12]. In the RGB color space, each component has a similarly distributed histogram. Thresholding R, G, and B components, the sky background is masked and the targets such as bridge and road pavement are focused, although trees and grass remain. In the L*a*b* color space, L* represents the brightness information of gray scale, and a*b* components represent the color information. The L*a*b* color space more flexibly achieved to mask sky, trees, and grass. This paper proposes a damage color segmentation based on the L*a*b* values to localize the target features such as infrastructures and damage for disaster monitoring (Fig. 3).

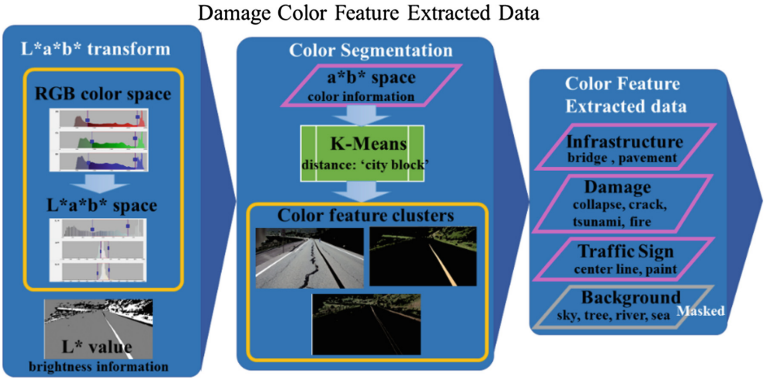


**Fig. 3.** Damage color segmentation based on the a*b* space using K-means clustering.

**Color-Base Augmentation Using Color Segmentation K-Means Clustering**
This paper presents a color-base augmentation using damage color segmentation, where the original images are transformed from the RGB to L*a*b* color space to take advantage of the fact that L*a*b* is one example of a device-independent color space. The L* value can represent the brightness with gray-scale information. The a*b* space can represent the color information. These values can act as the input for the K-means clustering algorithm for color-based segmentation. We can calculate these distances with color space similarity on neighbor pixels selecting whether the Euclidean or city block. In the case using the Euclidean distance to minimize a cost function, there were many calculation results that did not converge in the disaster image dataset. This paper proposes to use the city block distance between the center and any nearby points.

**Color-Base Damage Feature Categorization for Quake Disaster Monitoring**
The color-base region of interest (ROI) monitoring a disaster image is divided into four categories, namely (1) damaged infrastructure with earthquake disaster or (2) health infrastructure without disaster, (3) traffic sign, and (4) background. For example, the color-base ROI of health infrastructure is represented by bridge with concrete white color and road pavement is denoted by blue-colored asphalt (fresh pitch stone - rekisei) and faded into gray-colored. In detail, damaged infrastructure with disaster features are divided into two patterns, at first, the same color with disaster specific-shape (collapse, crack, curve like wave, break, and interruption). Second, the specific-color with damaged parts of infrastructure (road crack showing stratum underground with brown-color) and the background disaster-change (gray and black smoke, orange fire, tsunami black sea). The color-base ROI of traffic sign is denoted by the center line with orange-color, and the side line with white-color. That of background contains sky with light blue or cloudy white color, tree with green and brown-color, and river with blue and green-color, and ground with brown-color, these color corresponds to the temperature and time-range. Several color clusters (K = 2, 3, 4, 5) are segmented; these categorized images are used as an input of color feature extracted data for learning a damage classifier. In contrast, the parts of the background category are masked. These background color segmented images are not added to the original images as an input of a damage classifier, because the background color is not damaged signal but noise without enhancement.

### 2.3 Support Vector Damage Classifier

**Damage Feature Extraction using Pre-trained Deep Network: DenseNet-201**
Feature extraction is commonly used in machine learning applications. We can consider a pre-trained network and use it as an input feature to learn a classification task. Image classification using feature extraction is generally much faster and less computationally strenuous than the transfer learning process tuning weights and biases at deep layers. We can rapidly construct a classifier to a new task using an extracted feature at the concatenated layer as a training column vector [13]. This paper proposes a support vector classification model using a single layer from the concatenated feature extraction. Furthermore, we provide the classification model using multiple layers from several feature extractions at significant concatenated points. We can load pre-trained

networks such as AlexNet [14], GoogleNet [15], VGG16 and VGG19 [16], ResNet18, ResNet50 and ResNet101 [17], Inception v3 [18], Inception-ResNet-v2 [19], SqueezeNet [20] and DenseNet-201 [21]. Yasuno et al. have already compared feature extracted support vector classifiers based on above ten pre-trained architectures, where they found that DenseNet-201 based support vector classifiers had the best accuracy among the 10 models toward the disaster image dataset [22]. This paper proposes that the damage feature extraction using DenseNet-201 whose features under "conv5_block32_concat" concatenated layer are used as an input of the support vector classification model.

**Color-Base Damage Feature Enhanced Support Vector Classifier**

Let us suppose multiple disaster feature classes for a support vector classification model. In multiple classification models of more than two classes, we use a voting strategy [23–25]: each binary classification is considered to be a vote where votes can be for all data points in the end. The point is designated to be in a class with the maximum number of votes. The rapid library, LIBSVM, implements the one-against-one approach for multi-class classification. Many other methods are available for the multi-class support vector classification [23–25]. This study uses the kernel of a radial basis function with parameter gamma. In the case of image classifications, the number of extracted features is always a large number. In this study, there is a maximum instance whose number of disaster feature column vectors is 89,736 elements. In the case of an earthquake damage dataset we used, the support vector classification method confirmed the preferred advantage concerning both faster and accurate computation compared with other classification methods such as k-nearest neighbors, decision trees, random forests, and boosting methods. This study constructs a support vector classifier using damage color extracted features based on DenseNet-201 pre-trained networks (Fig. 4).

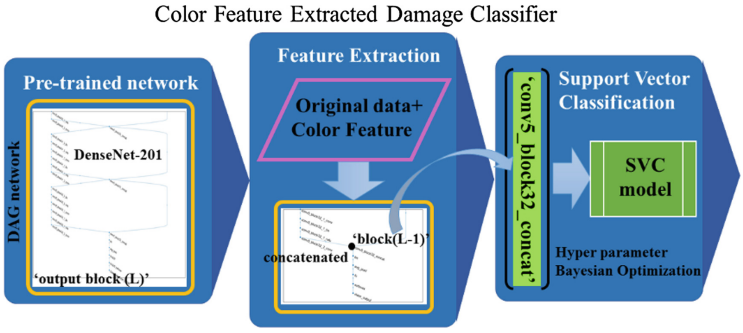


**Fig. 4.** Feature extraction enhanced with damage color and support vector classifier optimization.

**Hyper Parameter Bayesian Optimization Method for Damage Classifier**

There exists automated machine learning methods that use Bayesian optimization to tune hyper parameters of the machine learning pipeline. We can implement some libraries such as Auto-WEKA, auto-sklearn, and Auto-Model [26–28]. Grid search and

randomized search do not use the information produced from previous training runs; this is a disadvantage not encountered with Bayesian-based optimization methods. Bayesian-based optimization methods leverage the information of previous training runs to determine the hyper parameter values for the next training run and navigate through the hyper parameter space in a more efficient manner. The basic idea of warm start is to use the information gained from previous training runs to identify smarter starting points for the next training run. When building machine learning models, a loss function helps in minimizing the prediction error during the training phase. This paper proposes a Bayesian optimization method whose objective function is a loss function from five-fold cross validation to minimize the classification error using a support vector classifier that contains input of extracted features based on a pre-trained network. As a standard setting, we propose that the support vector classification model is based on a radial basis kernel function with two hyper parameters such as a box constraint C and kernel scale gamma [23, 24]. This study attempts to find as many hyper parameters as possible as we can minimize the cross-validation loss function with 30 iterations using the Bayesian optimization method.

**Table 1.** Quake image original/augmented dataset and number of images within each class.

| Earthquake damage class | Number of original images | Number of color-base augmented images | Number of combined both images |
|---|---|---|---|
| Tsunami damage | 40 | 51 | 91 |
| Bridge collapse | 40 | 42 | 82 |
| Road damage with accident risk | 40 | 70 | 110 |
| Initial smoke and fire | 40 | 46 | 86 |
| Non-disaster | 40 | 43 | 83 |
| **Sum of five classes** | **200** | **252** | **452** |

## 3 Applied Results

### 3.1 Quake Disaster Image Dataset

We attempted to collect open source data from web pages where images of earthquake were available. The collective area made up of high-resolution earthquake disaster images is primarily based on large Japanese earthquake experiences such as the Great Hanshin Earthquake (1995 Jan 17) and the Great East Japan Earthquake (2011 Mar 11). However, these areas are not limited only to Japan but areas whose images can be used worldwide. This paper highlights the four earthquake disaster features consisting of tsunami damage, bridge collapse, road damage with accident risk, and initial smoke and fire. Table 1 shows that the number of original images for each category is 40, resulting in a total dataset containing 200 earthquake disaster feature images. After damage color segmentation without background clusters such as sky, trees, and rivers, the number of each target color extracted cluster image is 51, 42, 70, 46, 43, such that the total number of images within the color extracted features dataset is 252. Therefore,

the number of each target damage feature image is 91, 82, 110, 86, 83, resulting in a total usable dataset of 452 images. The total images are partitioned into training dataset and test dataset with rate 7 and 3, respectively. In order to compare the original data and the damage color added data, a test dataset consisting of 60 images is used for both cases, which is calculated as 30% of the original dataset. The number of training data with the original data is 140 images; this number is 70% of 200. Meanwhile, the total number of training data with added color extracted data with the original data is 316 images; this number is 70% of 452.

### 3.2 Color-Base Augmentation Using Damage Feature Extraction

In the following, the quake image dataset is applied to the color segmentation method using the K-means clustering algorithm. We indicated some color cluster images corresponding to each category such as background, infrastructure, road damage, smoke and fire, and tsunami on the following images.

**Background Color Feature Extraction**
*Sky, Tree, River Feature* (Fig. 5).

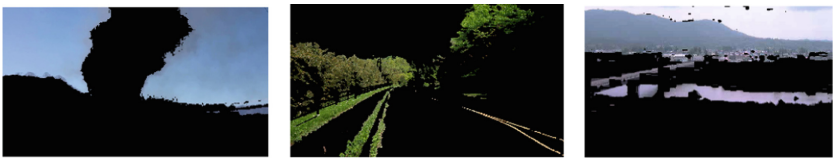

**Fig. 5.** Background color segmentation K-means clustering results.

**Health Infrastructure Color Feature Extraction (Non-disaster)**
*Road Pavement, Bridge Feature* (Fig. 6).

**Fig. 6.** Infrastructure color segmentation K-means clustering results.

**Traffic Sign Color Feature Extraction**
*Center line, Sidewalk line* (Fig. 7).

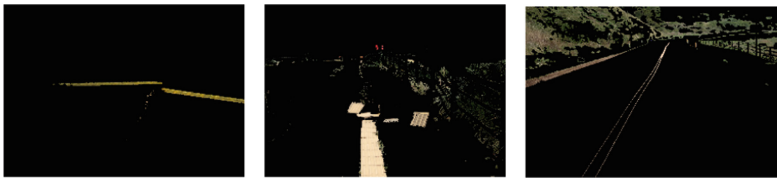

**Fig. 7.** Broken and curved traffic sign color segmentation K-means clustering results.

**Damaged Infrastructure Color Feature Extraction**
*Bridge Collapse Feature* (Fig. 8).

**Fig. 8.** Bridge collapse and interruption color segmentation K-means clustering results.

*Road Damage Color Feature* (Fig. 9).

**Fig. 9.** Crack and stratum color segmentation K-means clustering results.

*Smoke and Fire Color Feature* (Fig. 10).

**Fig. 10.** Smoke and fire color segmentation K-means clustering results.

*Tsunami Color Feature* (Fig. 11).

**Fig. 11.** Wave with splash color segmentation K-means clustering results.

### 3.3 Quake Damage Classifier Prediction Results

**Classification Results Using Color-Base Augmentation**

On the first row of Table 2, we show a result where input features with 89,736 values were extracted based on DenseNet-201 under "conv5_block32_concat." The feature inputs are computed to optimize hyper parameters for support vector classifiers, resulting in an accuracy improvement of 96.67%. The minimum objective function value is 0.0429. The process had a duration of 16 min 17 s during five-fold cross-validation iterations. On the second row of Table 2, we show a result where input features were extracted based on DenseNet-201 under the same concatenated layer, and the feature inputs are computed to optimize hyper parameters for support vector classifiers, resulting in an accuracy improvement of 98.68% more than previous original case. The minimum objective function value is 0.0568. The process has a duration of 16 min 50 s during five-fold cross-validation iterations. Thus, the color-base augmentation enhanced damage features is possible to improve the accuracy of the hyper parameter optimized support vector classifier using an earthquake damage dataset.

**Table 2.** Hyper parameter optimized results of support vector classifiers under an input of extracted features using pre-trained DenseNet-201.

| Input data | Feature extraction under pre-trained network | Hyper parameter optimized classifier |
|---|---|---|
| Original images #200 | DenseNet-201<br>"conv5_block32":<br>#89,736 | Objective function:<br>**0.0429**<br>Box constraint C: 0.0010<br>Rbf kernel scale: 0.0190<br>Training run time:<br>16 min 17 s<br>**96.67%** |
| Color-base augmentation added damage feature extracted images #452 | DenseNet-201<br>"conv5_block32":<br>#89,736 | Objective function:<br>**0.0568**<br>Box constraint C: 0.0298<br>Rbf kernel scale: 0.0112<br>Training run time:<br>16 min 50 s<br>**98.68%** |

Note: The objective function denotes the five-fold cross validation function value.

Figure 12 shows a hyper parameter optimization process of support vector classifier based on DenseNet-201 extracted single feature "conv5_block32_concat" layer. After three iterations, the loss function minimized at the stable level around 0.042.

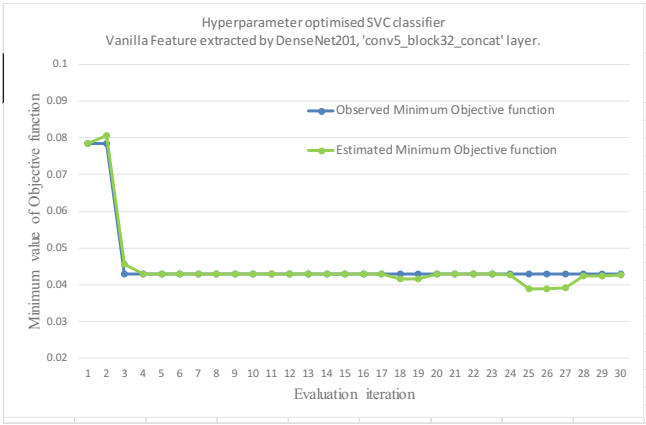


**Fig. 12.** Original image dataset (#200): hyper parameter optimization process of support vector classifier based on DenseNet-201 extracted single feature "conv5_block32_concat" layer.

Figure 13 shows a hyper parameter optimization process of support vector classifier based on DenseNet-201 extracted single feature "conv5_block32_concat" layer. After two iterations, the loss function minimized at the stable level around 0.056.

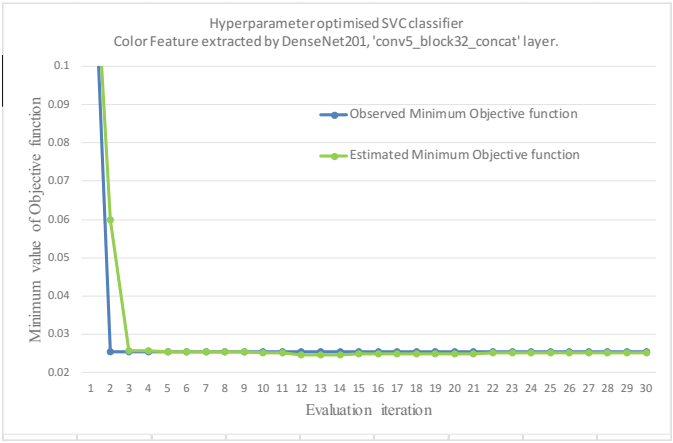


**Fig. 13.** Color-base augmentation added with original image dataset (#452): hyper parameter optimization process of support vector classifier based on DenseNet-201 extracted above layer.

Figure 14 shows the estimated minimum objective function value at the hyper parameter optimization process of support vector classifier. Although the minimized value under the original data (green line) warm starts, but after two iterations, the objective function value under the color-base augmentation (red line) maintains smaller level than the original one. Thus, this indicates that color-base augmentation has advantages with regard to accuracy and fast minimization for hyper parameter optimization.

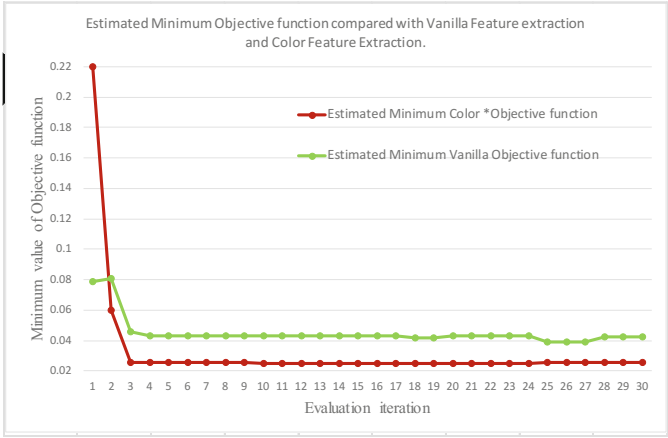


**Fig. 14.** Comparison of estimated objective functions of the original image data and the color image enhanced with the original image dataset: hyper parameter optimization process of support vector classifier based on DenseNet-201 (Color figure online)

### Confusion Matrix Under Damage Color Classifier

Table 3 shows the confusion matrix of a hyper parameter optimized support vector classifier extracted feature "conv5_block32_concat" layer based on DenseNet-201.

**Table 3.** Confusion matrix of hyper parameter optimized support vector classifier extracted feature based on DenseNet-201; the original data training (left), and the damage color feature added with original data (right).

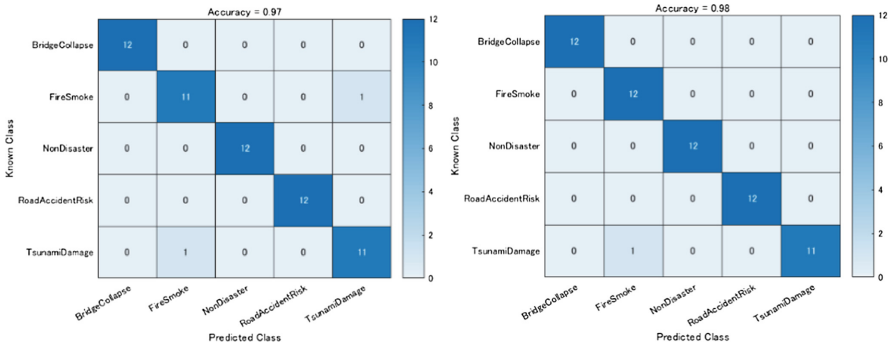

# 4 Concluding Remarks

## 4.1 Color Imaging Applications for Quake Disaster Monitoring

This paper presented a method to enhance the damage color feature extracted based on an object suited deep architecture DenseNet-201 in order to classify five classes of quake damage: tsunami, bridge collapse, road crack with accident risk, and smoke and fire. The training data were based on original images combined with added damage color features to incorporate the enhancement of several target features without other masked regions such as the sky, trees, and rivers. This support vector classifier containing a radial basis kernel function, the image classification model were Bayesian optimized to minimize the loss function with five-fold cross-validation. This method was applied to a case study of an earthquake image dataset whose total number was 452 examples with 89,736 color features. The first study using the original images were carried out with an accuracy of 96.67%, whereas the second study using the original and damage color extracted images achieved a more accurate rate of 98.68%. The loss function was also minimized faster and at a stable level. Therefore, it can be concluded that damage color extraction has advantages with regard to accuracy and fast minimization for hyper parameter optimization.

## 4.2 Future Works for Disaster Color Monitoring

The earthquake image dataset has 1,117 examples; therefore, we will attempt to apply this proposed method with color enhancement. Here, it is important to automate the hyper parameter K based on K-means clustering and an autonomous color segmentation; i.e., whether each color cluster corresponds to a damage class or not. We will tackle the problem thresholding color components under the a*b*space. We will investigate further opportunities regarding disaster damage classification for not only earthquake damage features but also other disaster features such as strong winds [31], building break down [32], traffic signal black out, and heavy rain and flood [33]. Disasters such as fire and flood are likely to occur more frequently when compared to earthquakes. This proposed color enhanced classifier could enable targeted disaster surveillance within each region, learning thousands of damage color features. It would take considerable time to collect newly damaged color data. We will continue to collect video data after the occurrence of any large earthquake worldwide to incorporate novel damage color variations not yet experienced. Such data mining of damage colors could contribute to better decision-making and prioritization of deploying an initial response to damaged infrastructure.

**Acknowledgements.** We wish to thank the CCIW committee and referees for their thoughtful comments. We would like to thank Fukumoto Takuji and Kuramoto Shinichi (MathWorks Japan) for providing us useful information on the MATLAB resources: the Image Processing, Machine Learning, and Parallel Computing. We also wish to thank Yachiyo Engineering Co., Ltd. for various supports.

## References


1. Manzhu, Y., Chaowei, Y., Yun, L.: Big data in natural disaster management: a review. Geosciences **8**, 165 (2018)
2. Michel, U., Thunig, H., Reinartz, P.: Rapid change detection algorithm for disaster management. ISPRS Ann. Photogramm. Remote Sens. Spat. Inf. Sci. **1–4** (2012)
3. Singh, A.: Review article digital change detection techniques using remotely-sensed data. Int. J. Remote Sens. **10**(6), 989–1003 (1989)
4. Saptarsi, G., Sanjay, C., Sanhita, G., et al.: A review on application on data mining techniques to combat natural disasters. Ain Shams Eng. J. **9**(3), 365–378 (2018)
5. Sakaki, T., Okazaki, M., Matsuo, Y.: Earthquake shakes Twitter users: real-time event detection by social sensors. In: Proceedings of 19th International Conference on World Wide Web. ACM (2010)
6. Chitade, A., Katiyar, S.K.: Color based image segmentation using K-means clustering. Int. J. Eng. Sci. Technol. **2**(10), 5319–5325 (2010)
7. Shmmala, F., Ashour, W.: Color based image segmentation using different versions of K-means in two spaces. Glob. Adv. Res. J. Eng. Technol. Innov. **1**(9), 30–41 (2013)
8. Hassan, R., Ema, R., Islam, T.: Color image segmentation using automated K-means clustering with RGB and HSV color spaces. Glob. J. Comput. Sci. Technol. F Graph. Vis. **17** (2) (2017)
9. National Oceanic and Atmospheric Administration (NOAA) Homepage, Natural Hazards Image Database, Events contains Earthquake, Tsunami, Volcano, and Geology. https://www.ngdc.noaa.gov/hazardimages/earthquake. Accessed 17 Sept 2018
10. Sharma, G.: Digital Color Imaging Handbook. CRC Press, Boca Raton (2003)
11. Gonzalez, R., Woods, R., Eddins, S.: Digital Image Processing Using MATLAB, 2nd edn. McGrawHill Education, New York (2015)
12. The Great Hanshin Awaji Earthquake 1.17 Records, Kobe City Homepage, open photo data. http://kobe117shinsai.jp/. Accessed 27 Oct 2018
13. Aurelien, G.: Hands-On Machine Learning with Scikit-Learn and TensorFlow: Concepts, Tools, and Techniques to Build Intelligent Systems. O'Reilly Media Inc., Sebastopol (2017)
14. Krizhevsky, A., Ilya, S., Hinton, G.E.: ImageNet classification with deep convolutional neural networks. In: Advances in Neural Information Processing Systems (2012)
15. Szegedy, C., Wei, L., Yangqing, J., et al.: Going deeper with convolutions. In: Proceedings of the IEEE Conference on Computer Vision and Pattern Recognition, pp. 1–9 (2015)
16. Simoniyan, K., Zisserman, A.: Very deep convolutional networks for large-scale image recognition. In: ICLR. VGG model, the Visual Geometry Group at University of Oxford (2015)
17. Kaiming, H., Xiangyu, Z., Shaoqing, R., et al.: Deep residual learning for image recognition. ResNet model. arXiv:1512.03385v1 (2015)
18. Szegedy, C., Vincent, V., Sergey, I., et al.: Rethinking the inception architecture for computer vision. In: CVPR, pp. 2818–2826. Inception v3 model (2015)
19. Szegedy, C., Sergey, I., Vincent, V., et al.: Inception-v4, Inception-ResNet impact of residual connections on learning. Inception-ResNet-v2 model. arXiv:1602.07261v2 (2016)
20. Forrest, N.I., Song, H., Matthew, W., et al.: SqueezeNet: AlexNet-level accuracy with 50x fewer parameters and < 0.5 MB model size. In: ICLR (2017)
21. Huang, H., Liu, Z., Maaten, L., et al.: Densely connected convolutional networks. In: CVPR (2017). DenseNet model

22. Yasuno, T., Amakata, M., Fujii, J., Shimamoto, Y.: Disaster initial response mining damages using feature extraction and bayesian optimised support vector classifier. In: 3rd International Conference on Data Mining & Knowledge Management, Dubai (2018)
23. Scholkopf, B., Smola, A.J.: Learning with Kernels: Support Vector Machines, Regularization, Optimization, and Beyond. MIT Press, Cambridge (2002)
24. Hsu, C.-W., Chang, C.-C., Lin, C.-J.: A practical guide to support vector classification. Technical report, Department of Computer Science, National Taiwan University (2003)
25. Chan, C.-C., Lin, C.-J.: LIBSVM: a library for support vector machines, pp. 29–30 (2013). Initial version 2001, Multi-class classification
26. Feurer, M., Klein, A., Eggensperger, K.: Efficient and robust automated machine learning. In: Neural Information Processing Systems Conference (NIPS) (2015)
27. Sergios, T.: Machine Learning: A Bayesian and Optimization Perspective. Academic Press, Cambridge (2015)
28. Sibanjan, D., Cakmak, U.M.: Hands-On Automated Machine Learning, Packt (2018)
29. Prince, S.: Computer Vision Models, Learning, and Inference. Cambridge University Press, Cambridge (2017)
30. Rajalingappaa, S.: Deep Learning for Computer Vision, Packt (2018)
31. Yasuno, T.: Estimating occurrence probability and loss index to manage the social risk of storing-winds. In: International Symposium Society for Social Management Systems (SSMS) (2009)
32. Yasuno, T.: Daily interaction behavior, urgent support network on Tohoku Tsunami 2011, Tottori Quake 2000, Social Capital and Development Trends in Rural Areas, vol. 8, Chap. 12 (2012)
33. Takato, Y.: Dam inflow time series regression models minimising loss of hydropower opportunities. In: Ganji, M., Rashidi, L., Fung, B.C.M., Wang, C. (eds.) PAKDD 2018. LNCS (LNAI), vol. 11154, pp. 357–367. Springer, Cham (2018). https://doi.org/10.1007/978-3-030-04503-6_34